

An application of Gaussian regression and SURF method for Mexican history of painting

Liam Carpenter (lc3919)¹ and Mariana Martinez (mgm9745)²

Computational Statistics MA-6973

New York University

Instructor: Mike O'Neil (oneil@cims.nyu.edu)

Contents

1 About This Problem	3
1.1 Mexican Art History	3
1.1.1 Santiago Rebull (1829-1902)	3
1.1.2 José María Velasco (1840-1912)	3
1.1.3 Alfredo Ramos Martínez (1871-1946)	4
1.1.4 Gerardo Murillo, Dr Atl (1875-1964)	4
1.1.5 José Clemente Orozco (1883-1949)	4
1.1.6 Diego Rivera (1886-1957)	5
1.1.7 Rufino Tamayo (1899-1991)	5
1.1.8 Frida Kahlo (1907-1954)	6
1.1.9 Remedios Varo (1908-1963)	6
1.1.10 Javier Marín (1962)	7
1.2 Mexican Art Data Problem	7
1.3 Objective of this project	7
2 Introduction to Computer Vision	8
2.1 What is Computer Vision	8
2.2 Introduction to SURF	8
2.2.1 Integral Images	8
2.2.2 Interest Point Detection	9
2.2.3 Orientation Assignment	10
2.3 Descriptor Components	11
3 Introduction to Gaussian Processes	12
3.1 The Basics	12
3.2 Kernel functions	13
3.2.1 Squared exponential kernel	13
3.2.2 Exponential kernel	13
3.2.3 Matern kernel	13
3.2.4 Rational quadratic kernel	13
3.2.5 Kernels with separate length scale per predictor	14
3.3 Working With Data	14
4 Methodology	15
4.1 Data Base Used	15
4.2 Methodology	15
4.2.1 Transforming data	15
4.2.2 Fitting Gaussian regressions	16
4.3 Limitations and problems	16
5 Interpretation and Conclusions	17
5.1 Results	17
5.2 Example of painting analysis	19
5.3 Conclusions	20
5.4 Future analysis	20
6 Appendix A	22

1 About This Problem

The main idea behind this project is to explore the possibility of applying Gaussian regression to data extracted from paintings in order to predict the year those paintings were done. We are also interested on those paintings that are classified wrongly because it means that those paintings have certain stylistic similarities with paintings from another period in time. This problem is a central discussion in art history. So if a painting is not classified correctly and the correct year is before than the predicted year, it might mean that that particular painting could be considered "advanced" for its year. We want to explore the possibility of giving art historians more computational tools for their research.

1.1 Mexican Art History

We want to give the reader a brief summary on Mexican art history just for context. The paintings we used are from the late XIX century and all the XX century. This is because it was until the XX century when we can talk about Mexican art as we know it today. During the XIX most artists copied other styles from abroad, specially from France and the UK, as the reader can find in [7]. In this project we worked with 10 Mexican (or considered Mexican) artists. We want to give a small context derived from both Elizondo's and Ole's books [13, 16].

1.1.1 Santiago Rebull (1829-1902)

He's one of the most important painter of the XIX century and was Diego Rivera's professor. His family was mainly European so he could have the privilege of painting freely, specially religious paintings. His motifs are inspired in European traditions and history, as most paintings of this era.



La Muerte de Marat, Santiago Rebull

1.1.2 José María Velasco (1840-1912)

He is the most famous landscape painter in Mexico and his artwork is internationally renowned. He was a professor at the Mexican Academia and taught many of the most famous artists of the XX century.



Paisaje Mexicano, José María Velasco

1.1.3 Alfredo Ramos Martínez (1871-1946)

He's an important figure for the XXth century art in Mexico because in 1920 he founded schools called *Escuelas al Aire Libre de Santa Anita*. This was heavily influenced by European style of painting and teaching. But from this point on Mexican artists stood out internationally due to their different painting style, technique, and motifs.



Abrazo Materno, Alfredo Ramos Martínez

1.1.4 Gerardo Murillo, Dr Atl (1875-1964)

As most artists, he also studied abroad in Europe. He organized an art exhibit in 1910 when things were changing in the art world. Thanks to this exhibit Mexican art started to be notorious internationally.



Erupción en Apogeo, Dr. Atl

1.1.5 José Clemente Orozco (1883-1949)

He is considered to be one of the 3 greatest muralists of all time with Siqueiros and Rivera. His murals are spread all around the world (including New York City).



La Tierra, José Clemente Orozco

1.1.6 Diego Rivera (1886-1957)

Diego Rivera is probably one of the most outstanding Mexican artists of all time. He was in charge of starting the muralist movement as part of an education campaign. He is one of the very few artists in Mexico that experimented with a lot of styles (cubism, muralism, surrealism, abstraction, etc). This is why classifying his paintings is so hard.



Tres figuras, Diego Rivera

1.1.7 Rufino Tamayo (1899-1991)

Tamayo is one of the most famous painters in Mexico. His paintings are characterized by having a lot of texture thanks to the combination of paint and sand he used. He is one of the firsts to start painting Mexican motifs and everyday life in a combination of styles: cubism, surrealism, and abstract expressionism.



Las sandías, Rufino Tamayo

1.1.8 Frida Kahlo (1907-1954)

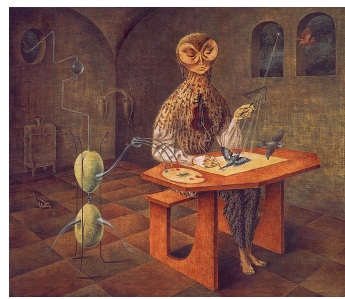
Frida Kahlo is the most well known Mexican artist in the world. Her life was full of tragedies and medical issues that she expressed in her paintings. She had polio, broke her spine in 3 pieces at an accident, had several unwanted abortions, and was immobilized for a period of time.



Las Dos Fridas, Frida Kahlo

1.1.9 Remedios Varo (1908-1963)

Varo was born in Spain but she fled during the Spanish Civil War and ended up in Mexico, where she finally became a citizen. Remedios Varo, Leonora Carrington, and Frida Kahlo shaped a great part of the late XX century painting style in Mexico and worldwide surrealism.



La Creación de las Aves, Remedios Varo

1.1.10 Javier Marin (1962)

The three Marin brothers are currently some of the most important contemporary artists alive in Mexico. He has done several exhibits across important museums worldwide such as the Museum of Fine Arts in Boston.



Cuatro Manos II, Javier Marin

1.2 Mexican Art Data Problem

One of the fundamental problem in Mexican art history (and hence a problem we've had in this project) is lack of data in different levels:

- Lack of dates when paintings were made: this is why we want to predict those dates but since there is lack of data, we can't use much data to train our models.
- Lack of HD images from the paintings themselves: there is currently no public data base containing "good" quality pictures of Mexican paintings. So most of the images used are from the same data base as [15], but that data base is currently under construction as well and that mainly feeds from information that can be found on [18, 14, 10, 11, 1, 2, 3, 4, 5].

1.3 Objective of this project

As the reader might notice, there are several technical problems in the world of Mexican art data. Some work has been done in trying to apply computational statistic method to help solve some questions in the world of art history. Some of those problems have to do with style classification as seen in [9, 8, 15]. In this project we wish to give an exploration using Gaussian regression to investigate the possibility of using such methods to help solving the problem of lack of dates when paintings were made. This has not been done before in the Mexican context so this is a first attempt to find possible paths for solutions.

2 Introduction to Computer Vision

2.1 What is Computer Vision

2.2 Introduction to SURF

In computer vision it is often useful to find and describe similarities between two images. Speeded Up Robust Features(SURF) is an approach proposed by Hebert et al. in [6] as scale and rotation invariant method to find points of interest in an image and construct informative features out of the neighborhoods of these points. The power of the SURF method over it's predecessors such as SIFT (Scale Invariant Feature Transform) is in its strong performance despite the approximations made to increase computational efficiency. There are two parts to this method:

1. Interest Point Detection
2. Description of the neighborhood of these interest points

2.2.1 Integral Images

The SURF method leans heavily on the use of a Data Structure known as an integral image, to compute sums over rectangular regions of an images pixel values quickly. An integral image is a transformation of image data, for example channel intensities of an RGB image, such that for an $n \times n$ image it will produce an $n \times n$ integral image where each entry of the integral image $I_{\Sigma}(\mathbf{x})$, corresponding to the coordinate pair $\mathbf{x} = (x, y)$, is the sum of all the pixel values above and to the left of that point inclusive. Formally, following the convention that an images coordinates start with $(0, 0)$ as the upper left most pixel, the entries of the integral images are computed according to:

$$I_{\Sigma}(\mathbf{x}) = \sum_{i=0}^x \sum_{j=0}^y I(i, j).$$

Here $I(i, j)$ represents the value of the pixel at coordinate (i, j) . This in turn reduces the computation of a sum over a rectangular region of pixel values to 4 addition and subtraction operations, irrespective of the size of that region. An example of how this can be used for efficient computation of the total sum of a boxed region is shown in figure 11.

1.	<table border="1"><tr><td>31</td><td>2</td><td>4</td><td>33</td><td>5</td><td>36</td></tr><tr><td>12</td><td>26</td><td>9</td><td>10</td><td>29</td><td>25</td></tr><tr><td>13</td><td>17</td><td>21</td><td>22</td><td>20</td><td>18</td></tr><tr><td>24</td><td>23</td><td>15</td><td>16</td><td>14</td><td>19</td></tr><tr><td>30</td><td>8</td><td>28</td><td>27</td><td>11</td><td>7</td></tr><tr><td>1</td><td>35</td><td>34</td><td>3</td><td>32</td><td>6</td></tr></table>	31	2	4	33	5	36	12	26	9	10	29	25	13	17	21	22	20	18	24	23	15	16	14	19	30	8	28	27	11	7	1	35	34	3	32	6
31	2	4	33	5	36																																
12	26	9	10	29	25																																
13	17	21	22	20	18																																
24	23	15	16	14	19																																
30	8	28	27	11	7																																
1	35	34	3	32	6																																
2.	<table border="1"><tr><td>31</td><td>33</td><td>37</td><td>70</td><td>75</td><td>111</td></tr><tr><td>43</td><td>71</td><td>84</td><td>127</td><td>161</td><td>222</td></tr><tr><td>56</td><td>101</td><td>135</td><td>200</td><td>254</td><td>333</td></tr><tr><td>80</td><td>148</td><td>197</td><td>278</td><td>346</td><td>444</td></tr><tr><td>110</td><td>186</td><td>263</td><td>371</td><td>450</td><td>555</td></tr><tr><td>111</td><td>222</td><td>333</td><td>444</td><td>555</td><td>666</td></tr></table> <p>$15 + 16 + 14 + 28 + 27 + 11 =$ $101 + 450 - 254 - 186 = 111$</p>	31	33	37	70	75	111	43	71	84	127	161	222	56	101	135	200	254	333	80	148	197	278	346	444	110	186	263	371	450	555	111	222	333	444	555	666
31	33	37	70	75	111																																
43	71	84	127	161	222																																
56	101	135	200	254	333																																
80	148	197	278	346	444																																
110	186	263	371	450	555																																
111	222	333	444	555	666																																

Figure 11

2.2.2 Interest Point Detection

First the SURF algorithm uses a Hessian based approach to score and identify points of interest. Importantly interest points should be detected across different scales corresponding to different levels of detail in the image. These scores should be normalized across scales to allow for multi-scale comparison. Traditionally different scales of an image are computed by convolving a discretized and cropped Gaussian kernels of increasing standard deviations σ over a boxed neighborhood of a point to create a hierarchy of resolutions getting "blurrier" or more granular as σ is increased. The Hessian is then computed at each scale σ of a point \mathbf{x} where $L_{xx}(\mathbf{x}, \sigma)$ corresponds to the convolution of the second derivative $\frac{\partial^2}{\partial x^2}g(\sigma)$ over a box around the point \mathbf{x} .

$$\mathcal{H}(\mathbf{x}, \sigma) = \begin{bmatrix} L_{xx}(\mathbf{x}, \sigma) & L_{xy}(\mathbf{x}, \sigma) \\ L_{yx}(\mathbf{x}, \sigma) & L_{yy}(\mathbf{x}, \sigma) \end{bmatrix}$$

The determinant of this Hessian is then used as a way to score points of interest, with greater values of the determinant being regarded as more important. The key insight of the SURF method is that these second order derivatives can be approximated crudely with box filters and subsequently computed very fast with integral images with comparable performance to other methods. The discretized and cropped versions of the second order partial derivatives of the Gaussians alongside the SURF approximations thereof are visualized in figure below taken from [20].

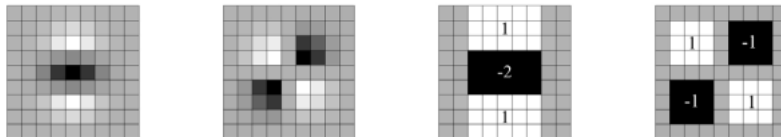


Figure 12: 9×9 filters corresponding to Gaussian discretized and cropped Gaussian second order partial derivatives and box filter approximations thereof.

We denote these approximations D_{xx}, D_{yy}, D_{xy} . The determinant needs to be further weighted to achieve good approximations, $\frac{|L_{xy}(1.2)|_F |D_{xx}(9)|_F}{|L_{xx}(1.2)|_F |D_{xy}(9)|_F} \approx .9$ where $|x|_F$ is the Frobenius norm, yielding,

$$\det(\mathcal{H}_{approx}) = D_{xx}D_{yy} - (0.9D_{xy})^2.$$

Filter responses are then normalized with respect to the filter size to guarantee a constant Frobenius norm across all filter sizes.

Generally, the scale spaces are implemented by repeatedly applying the same Gaussian filter to sub-sampled portions of the already filtered image creating the hierarchy of scales on which the interest points are computed. The SURF methods approximations allow this to be bypassed and instead each scale can be computed by up-scaling the filter size. The initial scale is the output of a 9×9 filter of scale $s = 1.2$ corresponding to Gaussian derivatives with $\sigma = 1.2$. The subsequent scales are computed with filters of size $15 \times 15, 21 \times 21, 27 \times 27$ and so forth. Each of these can be computed in constant time using the pre-computed integral images. The approximated Gaussian derivative scale multiplicatively with the filter size, ie. filter size 27×27 approximates the second order Gaussian derivative $\sigma = 3 \times 1.2 = 3.6 = s$.

2.2.3 Orientation Assignment

In order for the features produced to be invariant to rotation of the images, a reproducible orientation of the interest points must be determined. This is done using Haar wavelets. The Haar wavelet responses are calculate in a circular region of radius $6s$ around the interest points, where s is the scale at which the interest point was detected (points in this region sampled, equispaced s). The length of the edges of the wavelet are scale dependent at $4s$. The wavelet responses are then weighted with a Gaussian($\sigma = 2.5s$) centered at the interest point. These wavelet responses give us gradient like information about the images, which inform us about the magnitude and direction of change in pixel values, while being computable quickly with integral images. The responses are represented as vectors with the response strength to the horizontal wavelet as the x-coordinate and the vertical wavelet as the y-coordinate. A sliding window of angle $\frac{\pi}{3}$ is then applied over the circular region, summing up the horizontal and vertical responses within the region, yielding a new vector. The vector among these with the greatest magnitude is then said to be the orientation of the interest point. The steps of orientation assignment are shown graphically in figure 13 taken from [19]

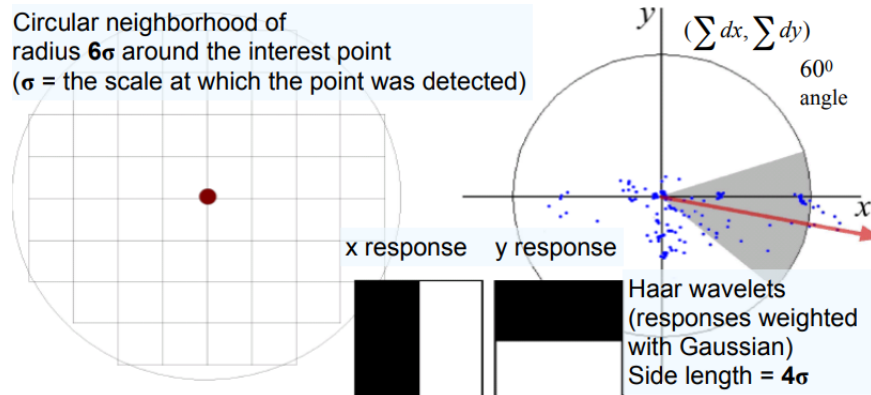


Figure 13: On the left the circular neighborhood over which the points are sampled, On the bottom are the horizontal and vertical wavelets used, on the right is the same circular region with the points corresponding to the wavelet responses weighted with a Gaussian and a $\frac{\pi}{3}$ slice of the region

2.3 Descriptor Components

Once the orientation has been fixed we need to come up with a descriptor. First a square region in the chosen orientation is constructed with side lengths $20s$. The regions are further partitioned into a 4×4 grid of sub-regions, with each sub-region sampled with a 5×5 grid of equispaced points. Once this is done the Haar wavelet response, with filter size of $2s$, is computed in the x and y directions relative to the orientation of the point. These responses are denoted d_x and d_y and are then weighted with a Gaussian centered at the interest point. Then the first set of features is constructed by summing up the responses d_x and d_y over each subregion. The next set of features is constructed by doing the same but on $|d_x|$ and $|d_y|$ resulting in a feature vector of $\mathbf{v} = (\sum d_x, \sum d_y, \sum |d_x|, \sum |d_y|)$. This results in a 4 dimensional feature vector for every one of the 16 sub regions. Giving us a 64 dimensional feature vector for every interest point. An example of how these features change for different images is given in the figure 14 taken from [6]

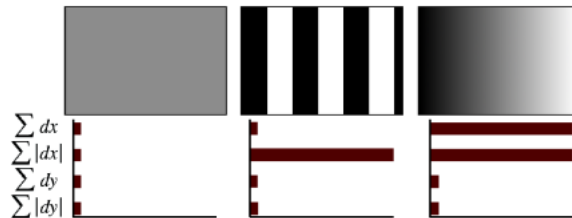


Figure 14

The final element included in the feature vector is the sign of the trace of the Hessian Matrix for the underlying interest point. This allows for some improvement in distinguishing lighter features on a dark background from dark features on a light background.

3 Introduction to Gaussian Processes

Once we have our features we would like to model their relationships over time using Gaussian processes. The essence of this approach falls within the Bayesian paradigm of modeling, where we fix a prior distribution representing our prior beliefs about the distribution that the data we have collected comes from. We then compute the joint distribution of our training points and test points according to the prior. Finally we compute the posterior distribution by conditioning on the observed variables. First we will define what a Gaussian Process is in the more general sense and then show how it can be applied to modeling observed data.

3.1 The Basics

In an introductory probability class one is introduced to the idea of a random variable which takes on different values dependent on the outcome of a random event. A Gaussian process is part of a larger family of stochastic processes that generalize the idea of a random variable to that of a random function, such that we can draw a function f from a distribution of functions and where each f is indexed by a variable t such that $f(t)$ is a random variable following some distribution.

Gaussian processes restrict this idea of a stochastic process such that all of the distributions under consideration are Gaussians. Formally a Gaussian Process is defined as a sequence $f(t_1) \dots f(t_n)$, where t_1, \dots, t_n is any collection of points, such that $f(t_1), \dots, f(t_n)$ is a multi-variate normal random vector, ie.

$$\begin{pmatrix} f(t_1) \\ \vdots \\ f(t_n) \end{pmatrix} \sim \mathcal{N}(\bar{\mu}, \Sigma)$$

The mean and co-variance structure of a normal distribution give it its specific form, and give us the form of a class of functions we can use to parametrize our distribution and express our prior belief about the data. These functions are called the mean function and co-variance kernel. Of particular importance is the co-variance kernel, it determines the smoothness of the function and the range of the dependence between indexings of a realization of our Gaussian process. For a general k dimensional multi-variate normal random distribution. We know that the mean of this distribution is a just a vector $\mu \in \mathbb{R}^k$. So any function that maps the index variables to real numbers is a suitable mean function. The co-variance kernel on the other hand has more restrictive properties. We know that the covariance matrix $\Sigma \in \mathbb{R}^{k \times k}$ of a multivariate normal distribution satisfies two properties which we would like to also have in our co-variance kernel $k(s, t)$.

1. Σ is symmetric: $\Sigma_{i,j} = \Sigma_{j,i}$. So we would like $k(s, t) = k(t, s)$
2. Σ is positive definite: $\forall \mathbf{x} \in \mathbb{R}^k, \mathbf{x}^\top \Sigma \mathbf{x} > 0$. So we would like $\langle \phi, K\phi \rangle = \int \int \phi(x)k(x, y)\phi(y)dxdy > 0$

It is important to keep in mind that the mean and co-variance function are parameters chosen by the modeler to specify their beliefs about the nature of the mean and co-variance structure of the data they have. Once these functions have been specified we can then use our prior to model the data we have collected.

3.2 Kernel functions

In our "experiment" we fitted different Gaussian regressions with different types of kernel functions and different parameters. In this subsection we wish to give a insight on those different kernels as in Duvenaud and Rasmussen [12, 17].

3.2.1 Squared exponential kernel

This kernel has the following form:

$$K(x, \hat{x}) = \sigma^2 \exp \left\{ -\frac{(x - \hat{x})^2}{2l^2} \right\}.$$

This is one of the most commonly used kernels since it has "nice" properties such as: it can be integrated against most functions and every function in its prior has infinitely many derivatives. Here l determines how close x and \hat{x} have to be to influence each other, or more formally known as the characteristic length-scale of the process.

3.2.2 Exponential kernel

This kernel, as once might guess has the following form:

$$K(x, \hat{x}) = \sigma^2 \exp \left\{ -\frac{|x - \hat{x}|}{2l^2} \right\}$$

Where l is still the length-scale of the process. The difference is that, while the squared exponential kernel is \mathcal{C}^∞ , the exponential kernel is just \mathcal{C}^0 .

3.2.3 Matern kernel

The Matern kernels are one of the most important families of kernels as seen in lecture. They depend on the parameter ν and have the following structure:

$$K(x, \hat{x}) = \frac{2^{1-\nu}}{\Gamma(\nu)} \left(\frac{\sqrt{2\nu}|x - \hat{x}|}{l} \right)^\nu K_\nu \left(\frac{\sqrt{2\nu}|x - \hat{x}|}{l} \right),$$

where K_ν is the modified Bessel function of order ν .

3.2.4 Rational quadratic kernel

. Usually ν is chosen such that $\nu = p + \frac{1}{2}$ for some $p \in \mathbb{N}$. If this is the case, then the kernel can be written as a product of an exponential and a polynomial of order p , making numerical calculations "easier". In our experiment:

- If $\nu = \frac{3}{2}$ then the kernel can be written as:

$$K(x, \hat{x}) = \sigma^2 \left(1 + \frac{\sqrt{3}|x - \hat{x}|}{l} \right) \exp \left\{ -\frac{-\sqrt{3}|x - \hat{x}|}{l} \right\}$$

- If $\nu = \frac{5}{2}$ then the kernel can be written as:

$$K(x, \hat{x}) = \sigma^2 \left(1 + \frac{\sqrt{5}|x - \hat{x}|}{l} + \frac{5(x - \hat{x})^2}{3l^2} \right) \exp \left\{ -\frac{-\sqrt{5}|x - \hat{x}|}{l} \right\}$$

A nice property of this kernel is that if $\nu \rightarrow \infty$ then this function converges to the squared covariance function.

3.2.5 Kernels with separate length scale per predictor

As seen in the subsections above, l is the parameter that controls the length scale of the process. There are two ways of viewing this:

- Using the same length-scale for each predictor
- Use a separate length-scale for each predictor. These methods implement automatic relevance determination:

$$\begin{aligned} l_m &= \log \sigma_m & \text{form } m = 1, 2, \dots, d \\ l_{d+1} &\log \sigma_f & \text{otherwise} \end{aligned}$$

3.3 Working With Data

We will operate in the noisy, supervised, setting where we have training data $\mathcal{D} = \{x_i, y_i\}_{i=1}^n, x_i \in \mathbb{R}^k$ and test data $\mathcal{T} = \{x_i^*\}_{i=1}^{n^*}$ that we want to make predictions on. We assume the model generating the data is

$$y = f(x) + \epsilon, \quad \epsilon \sim \mathcal{N}(0, \sigma^2)$$

Given a mean function $m(x)$ and co-variance kernel $k(x_1, x_2)$. We collect all our training observations x_i into a matrix $\mathbf{X} \in \mathbb{R}^{n \times k}$, our y_i 's into \mathbf{y} and test data into a matrix $\mathbf{X}^* \in \mathbb{R}^{n^* \times k}$. Our prior distribution is then,

$$\mathbf{y} \sim \mathcal{N}(\bar{0}, k(\mathbf{X}, \mathbf{X}) + \sigma^2 \mathbf{I})$$

Where we are using a 0 mean Gaussian for simplicity since a Gaussian $X \sim \mathcal{N}(\mu, \Sigma)$ can always be written as $X + \mu, X \sim \mathcal{N}(0, \Sigma)$. Then our joint distribution is

$$\begin{pmatrix} \mathbf{y} \\ \mathbf{y}^* \end{pmatrix} \sim \mathcal{N}(\bar{0}, \begin{pmatrix} K(\mathbf{X}, \mathbf{X}) + \sigma^2 \mathbf{I} & K(\mathbf{X}, \mathbf{X}^*) \\ K(\mathbf{X}^*, \mathbf{X}) & K(\mathbf{X}^*, \mathbf{X}^*) \end{pmatrix})$$

From this we can compute the posterior by conditioning on the observed data and noting that the posterior will have to be Gaussian to get

$$\mathbf{y}^* | \mathbf{X}^*, \mathbf{X}, \mathbf{y} \sim \mathcal{N}(K(\mathbf{X}^*, \mathbf{X})(K(\mathbf{X}, \mathbf{X}) + \sigma^2 \mathbf{I})^{-1} \mathbf{y}, K(\mathbf{X}^*, \mathbf{X}^*) - K(\mathbf{X}^*, \mathbf{X})(K(\mathbf{X}, \mathbf{X}) + \sigma^2 \mathbf{I})^{-1} K(\mathbf{X}^*, \mathbf{X}^*))$$

We then get a Bayesian estimator at our test points of $\mathbf{y}^* = K(\mathbf{X}^*, \mathbf{X})(K(\mathbf{X}, \mathbf{X}) + \sigma^2 \mathbf{I})^{-1} \mathbf{y}$

4 Methodology

4.1 Data Base Used

As stated in the first section, the main problem we've had is lack of data. So we worked with 160 paintings from 10 different artists as a training set and then with 27 paintings from those 10 artists as a test set. The amount of paintings per artists and the years they cover are the following:

Artist	Number of paintings used	Years covered
Santiago Rebull	2	1851-1875
José María Velasco	11	1840-1898
Alfredo Ramos Martínez	16	1929-1945
Gerardo Murillo	17	1908-1962
José Clemente Orozco	16	1925-1949
Diego Rivera	30	1907-1957
Rufino Tamayo	26	1934-1991
Frida Kahlo	19	1925-1954
Remedios Varo	16	1935-1963
Javier Marín	7	1987-2002

Table 1: Paintings and years per artist in the training set

This information comes from a data base which is still under construction due to the difficulty of finding this type of data and putting it together.

4.2 Methodology

This project can be divided into 3 main steps: transforming the images to vectors, fitting different Gaussian regressions, and analyzing those results.

4.2.1 Transforming data

As the reader might have already guessed, we used the SURF method in order to get numerical vector information from the pictures of the paintings. So for each color channel (red, green, and blue) and for each painting we extracted information in different ways:

- SURF point information: we extracted the 4 most important SURF points and then concatenated this information into a vector (per painting) that included their location, metric, scale, and sign of laplacian (then this vectors were of size 20).
- SURF point information and PCA: using the SURF point information described above we used PCA to reduce their dimension to vectors of size 5.
- SURF point features: after extracting the 4 most important SURF points we then calculated their features. So for each painting we had a 4 vectors of size 64.
- SURF point features and PCA: we wanted to reduce the dimension of those 64 size vectors so for all of them we used PCA and ended up with vectors of size 5.

4.2.2 Fitting Gaussian regressions

After getting our data vectors in order we fit different Gaussian regressions using different parameters. We do this because this is an exploration and we wish to try out different kernels and optimization methods to see what happens. The different optimization methods used are:

- Quasi-Newton: Newton's method with an approximation to the Hessian matrix.
- L-BFGS: also called limited-memory with BFGS updates of the Hessian.

The different kernels that were considered are the following:

- Exponential kernel
- Matern kernel with parameter 3/2
- Matern kernel with parameter 5/2
- Rational quadratic kernel
- Exponential kernel with a separate length scale per predictor
- Squared exponential kernel with a separate length scale per predictor
- Matern kernel with parameter 3/2 and a separate length scale per predictor
- Matern kernel with parameter 5/2 and a separate length scale per predictor
- Rational quadratic kernel with a separate length scale per predictor

4.3 Limitations and problems

There were a few limitations with the data base and some problems we've encountered in the making of this project:

- Lack of data, as stated before and lack of certainty of accuracy on the data we have. There is no way of proving these are the actual years these paintings were done.
- There are no other projects that are similar in style of what we've done here (at least that work with Mexican art) so there is no path set up to follow.

The reason why we ended up with 18 models per color channel per method of extraction of data is because we saw terrible l_∞ errors in our results (as seen in Appendix A in 6). But then we noticed that the average absolute error per method is almost the same for all of them and that it is much lower than the l_∞ errors. So we were interested in comparing errors derived from different norms as well.

5 Interpretation and Conclusions

5.1 Results

After fitting the 18 models per color channel per method of extraction of information we calculated different types of errors for both the training and test sets:

- l_2 error or the usual norm 2 of the absolute error vector.
- l_∞ error in the training set or the maximum of the absolute error vector.
- Average of all the entries on the absolute error vector.
- Average interval length (from the Gaussian regression).
- The number of the painting whose error corresponds to the l_∞ error.
- Percentage of paintings whose prediction error is smaller than the average prediction error.

We also calculated the time taken for the computer to run each of the experiments. The complete table with all this information can be found on Appendix A (on 6).

Throughout the different channels we have roughly similar errors. The minimum of the averages of the absolute errors in the test set is 16.855 and the maximum is 28.026 which we don't consider as bad since we don't have a lot of data and we are considering artwork coming from 1851 all the way to 2002. An interesting question arises when we look at the l_∞ norm of the absolute errors (which is always between 62.138 and 92.325 in the test set) and compare this with the average absolute error. Are there outliers? Is it more difficult to predict certain paintings year in comparison to others? These questions become even more interesting when we look at the following histograms:

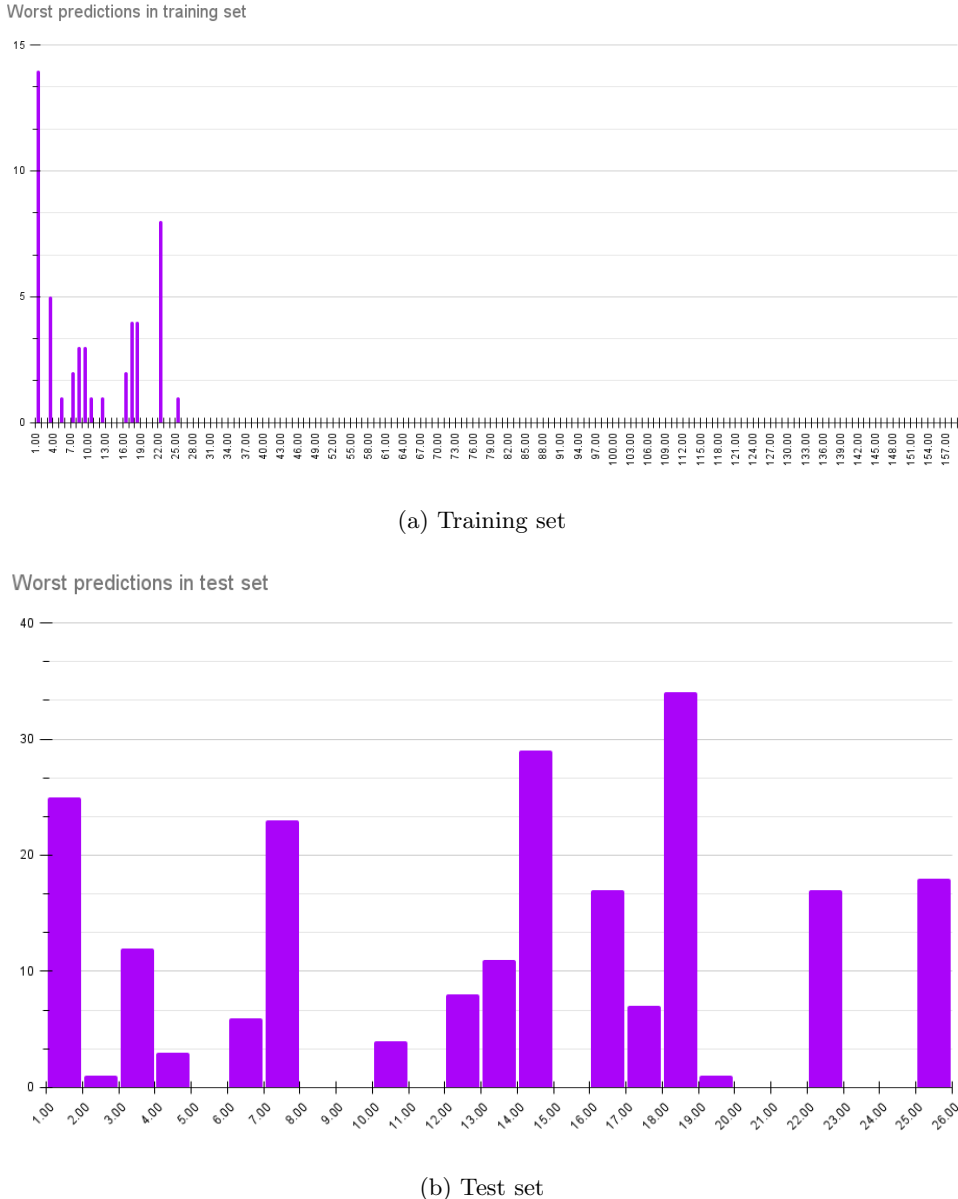


Figure 15: Painting number with the worst errors per model

We can conclude that there are some paintings whose year of creation is harder to predict than others. Since we can know which paintings these are (we have numbered them) we can proceed to do an analysis on one of them as an example of what can be done with these type of results.

5.2 Example of painting analysis

The painting that was incorrectly classified the most on the test set is painting number 18. This painting is the following one:



Figure 16: Bailarinas, Diego Rivera, 1939, gouache on rice paper 38.6 × 28 cm

Another examples of paintings that were done in 1939 are the following:



Figure 17: Example of paintings done in 1939

From figure 17 we can tell the different styles that artists experimented with in 1939. The

things that is common on this paintings is that there are different elements in them: texture, several composite figures, composite backgrounds, details, etc. But *Bailarinas* by Diego Rivera is a painting with just two "simple" figures and a simple yellow background. The SURF method relies on wavelet transforms and these transformations are good for detecting patterns, edges, and fine details. So it makes sense that this method can't detect much of them in figure 16 because Rivera painted simple figures.

5.3 Conclusions

It is difficult trying out computational methods in an artistic context because we had no background on what would happen here. Hence doing explorations like this is interesting. There is no intention from us to say that computational tools should replace the work of art historians. On the contrary, we believe that these type of analysis are helpful for them because they probably throw out unexpected results that are derived from a "objective" method.

5.4 Future analysis

As more data is gathered and verified (by art historians) there are different type of analysis that could be done, some of them are:

- Consider longer periods of time and more artists to train the Gaussian process with
- Try out different ways of getting image features from the paintings
- Fit Gaussian processes for certain style of painting or certain school exclusively

Bibliography

- [1] Artsy. URL: <https://www.artsy.net/>.
- [2] Philadelphia Museum of Art. URL: <https://philamuseum.org/>.
- [3] Casa de subastas Morton. URL: <https://www.mortonsubastas.com/>.
- [4] Sotheby's. URL: <https://www.sothbys.com/en/>.
- [5] Christie's Auctions. URL: https://www.christies.com/?sc_lang=en&lid=1.
- [6] Herbert Bay, Tinne Tuytelaars, and Luc Van Gool. "SURF: Speeded Up Robust Features". In: ().
- [7] "Catálogo de exposición: 1910, el arte en un año decisivo". In: (1989), p. 27.
- [8] Ingrid Daubechies et al. "Image Processing for Artist Identification". In: *IEEE Signal Processing Magazine* (2008).
- [9] Ingrid Daubechies et al. "Stylistic Analysis of Paintings Using Wavelets and Machine Learning". In: () .
- [10] Dr Atl. Inverarte. URL: <https://inverarteartgallery.com/artist/dr-atl/>.
- [11] Dr Atl el hechicero y pintor amante de los volcanes. Fahrenheit Magazine. URL: <https://fahrenheitmagazine.com/arte/dr-atl-el-hechicero-y-pintor-amante-de-los-volcanes>.
- [12] David Duvenaud. *Kernel Cookbook*. URL: <https://www.cs.toronto.edu/~duvenaud/cookbook/>.
- [13] Lupina Lara Elizondo, ed. *250 Artistas Mexicanos Siglos XIX, XX y XXI*. Promoción de Arte Mexicano, p. 272. ISBN: 978-607-7714-27-9.
- [14] Mariana Gaxiola. *Fantásticas obras para recordar a Dr. Atl*. MXCity. URL: <https://mxcity.mx/2017/10/obras-para-remembrar-dr-atl/>.
- [15] Mariana Martínez. "Una aplicación de ondículas al estudio de estilos de artistas plásticos mexicanos". 2021, p. 164.
- [16] James Oles. *Arte y arquitectura en México*. Taurus. ISBN: 978-607-113-193-5.
- [17] C.E. Rasmussen. *Gaussian Processes for Machine Learning*. MIT Press, p. 266. ISBN: 026218253X.
- [18] *Selected Paintings and Drawings 1930s and 1940s*. The Alfredo Ramos Martínez Research Project. URL: <https://www.alfredoramosmartinez.com/paintings-and-drawings>.
- [19] Mohammad Nayeem Teli. *Speeded Up Robust Features*. 2020. URL: https://www.cs.umd.edu/class/spring2020/cmsc426-0201/files/14_SURF.pdf.
- [20] Deepanshu Tyagi. *Introduction to SURF (Speeded-Up Robust Features)*. 2019. URL: <https://medium.com/data-breach/introduction-to-surf-speeded-up-robust-features-c7396d6e7c4e>. (accesado: 15.03.2021).

6 Appendix A

In this appendix we show the errors for each channel and for each method used. The columns are the following:

- L2 error training: the l_2 error in the training set or the usual norm 2 of the absolute error vector.
- Linf error training: the l_∞ error in the training set or the maximum of the absolute error vector.
- Error average training: the average of all the entries on the absolute error vector on the training set.
- Interval length average train: the average interval length (from the Gaussian regression) on the training set.
- Painting worst error training: the painting whose error corresponds to the l_∞ error in the training.
- Percentage paintings lower error than average train: the percentage of paintings whose prediction error is smaller than the average prediction error in the training set.
- L2 error test: the l_2 error in the test set or the usual norm 2 of the absolute error vector.
- Linf error test: the l_∞ error in the test set or the maximum of the absolute error vector.
- Error average test: the average of all the entries on the absolute error vector on the test set.
- Interval length average train: the average interval length (from the Gaussian regression) on the test set.
- Painting worst error test: the painting whose error corresponds to the l_∞ error in the test.
- Percentage paintings lower error than average train: the percentage of paintings whose prediction error is smaller than the average prediction error in the test set.
- Time taken: time taken to fit the model and verify it.

	L2 error training	Linf error training	Error average training	L2 interval length train	Interval length average train	Painting worst error training	Percentage paintings lower error than average train	L2 error test	Linf error test	Error average test	L2 interval length test	Interval length average test	Painting worst error test	Percentage paintings lower error than average test	Time taken
exponential + quasinewton and Blue Features	0.071	0.011	0.002	1.540	1.539	160	0.661	295.880	73.185	20.837	107.800	107.010	16	0.673	1.289
exponential + lbfgs and Blue Features	0.071	0.011	0.002	1.538	1.536	151	0.661	295.880	73.185	20.837	107.800	107.010	16	0.673	1.208
matern32 + quasinewton and Blue Features	0.071	0.011	0.002	1.536	1.536	38	0.653	296.320	73.673	20.912	107.500	106.560	16	0.673	1.018
matern32 + lbfgs and Blue Features	0.071	0.011	0.002	1.536	1.536	34	0.653	296.320	73.673	20.912	107.500	106.560	16	0.673	1.024
matern52 + quasinewton and Blue Features	0.071	0.011	0.002	1.536	1.536	34	0.653	296.450	73.567	20.921	107.39	106.420	16	0.673	0.957
matern52 + lbfgs and Blue Features	0.071	0.011	0.002	1.536	1.536	34	0.653	296.450	73.567	20.921	107.390	106.420	16	0.673	1.007
rationalquadratic + quasinewton and Blue Features	0.071	0.011	0.002	1.536	1.536	16	0.652	296.600	72.475	20.897	107.130	106.140	16	0.663	1.586
rationalquadratic + lbfgs and Blue Features	0.071	0.011	0.002	1.536	1.536	43	0.652	296.600	72.475	20.897	107.130	106.140	16	0.663	1.340
ardexponential + quasinewton and Blue Features	0.075	0.011	0.002	1.536	1.536	28	0.616	316.380	88.915	22.625	108.500	101.340	3	0.625	113.320
ardexponential + lbfgs and Blue Features	0.074	0.011	0.002	1.536	1.536	28	0.648	305.520	73.208	22.284	107.250	102.460	4	0.596	123.880
ardsquaredexponential + quasinewton and Blue Features	0.077	0.012	0.002	1.536	1.536	107	0.641	308.870	83.984	22.390	105.650	99.205	4	0.654	147.070
ardsquaredexponential + lbfgs and Blue Features	0.078	0.012	0.002	1.536	1.536	84	0.622	327.220	80.624	22.980	105.760	99.752	18	0.625	71.251
ardmatern32 + quasinewton and Blue Features	0.076	0.012	0.002	1.536	1.536	28	0.645	308.190	77.877	21.867	108.190	100.180	3	0.615	122.510
ardmatern32 + lbfgs and Blue Features	0.076	0.011	0.002	1.536	1.536	28	0.636	312.450	88.335	22.465	107.320	100.150	10	0.615	499.730
ardmatern52 + quasinewton and Blue Features	0.076	0.013	0.002	1.536	1.536	28	0.652	313.900	89.268	22.842	106.950	100.470	4	0.625	96.975
ardmatern52 + lbfgs and Blue Features	0.075	0.012	0.002	1.536	1.536	28	0.653	299.930	68.160	21.757	106.320	101.820	3	0.644	66.441
ardrationalquadratic + quasinewton and Blue Features	0.078	0.012	0.002	1.536	1.536	25	0.628	313.070	82.938	22.441	107.300	99.330	3	0.625	147.370
ardrationalquadratic + lbfgs and Blue Features	0.080	0.011	0.002	1.536	1.536	28	0.623	317.440	78.621	22.928	107.440	100.400	3	0.615	102.770
exponential + quasinewton and Blue Points	2.385	0.692	0.132	12.645	12.644	16	0.663	148.120	66.640	20.788	108.530	108.530	7	0.692	0.368
exponential + lbfgs and Blue Points	0.035	0.010	0.002	1.581	1.543	157	0.663	148.120	66.640	20.788	108.530	108.530	7	0.692	0.417
matern32 + quasinewton and Blue Points	0.953	0.277	0.053	8.002	8.002	7	0.663	148.130	66.637	20.793	108.530	108.530	7	0.692	0.329
matern32 + lbfgs and Blue Points	0.038	0.011	0.002	1.591	1.591	10	0.663	148.130	66.637	20.793	108.530	108.530	7	0.692	0.339
matern52 + quasinewton and Blue Points	1.379	0.400	0.076	9.621	9.621	9	0.663	148.140	66.637	20.797	108.520	108.520	7	0.692	0.312
matern52 + lbfgs and Blue Points	0.035	0.010	0.002	1.540	1.540	104	0.663	148.140	66.637	20.797	108.520	108.520	7	0.692	0.331
rationalquadratic + quasinewton and Blue Points	350.190	101.640	19.348	108.530	108.530	5	0.663	148.120	66.644	20.786	108.530	108.530	13	0.692	0.070
rationalquadratic + lbfgs and Blue Points	350.190	101.640	19.349	108.530	108.530	1	0.663	148.120	66.644	20.786	108.530	108.530	1	0.692	0.079
ardexponential + quasinewton and Blue Points	0.038	0.011	0.002	1.540	1.540	157	0.619	124.270	62.138	18.441	104.700	97.535	10	0.538	0.738
ardexponential + lbfgs and Blue Points	0.038	0.011	0.002	1.540	1.540	12	0.619	125.000	62.219	18.569	104.900	97.539	10	0.538	1.010
ardsquaredexponential + quasinewton and Blue Points	0.046	0.012	0.003	1.540	1.540	18	0.606	140.800	65.992	21.178	106.970	91.288	3	0.615	0.766
ardsquaredexponential + lbfgs and Blue Points	0.046	0.012	0.003	1.540	1.540	18	0.606	140.800	65.992	21.178	106.970	91.288	3	0.615	0.903
ardmatern32 + quasinewton and Blue Points	0.042	0.011	0.003	1.540	1.540	131	0.575	147.860	68.815	21.673	107.140	91.287	3	0.615	0.842
ardmatern32 + lbfgs and Blue Points	0.043	0.012	0.003	1.540	1.540	131	0.575	147.180	68.015	21.868	107.340	91.113	3	0.615	0.559
ardmatern52 + quasinewton and Blue Points	0.044	0.012	0.003	1.540	1.540	131	0.569	154.730	71.338	22.407	107.820	90.312	10	0.692	0.681
ardmatern52 + lbfgs and Blue Points	0.044	0.012	0.003	1.540	1.540	131	0.575	149.260	69.072	22.246	107.330	90.518	3	0.654	0.826
ardrationalquadratic + quasinewton and Blue Points	0.046	0.012	0.003	1.540	1.540	18	0.606	140.800	65.992	21.178	106.970	91.288	3	0.615	1.117
ardrationalquadratic + lbfgs and Blue Points	0.046	0.012	0.003	1.540	1.540	18	0.600	140.290	65.967	21.066	106.890	91.342	3	0.615	0.739
exponential + quasinewton and Blue PC Features	195.610	28.441	5.442	74.889	74.794	8	0.656	296.770	70.653	20.868	108.280	107.470	25	0.673	0.674
exponential + lbfgs and Blue PC Features	195.610	28.441	5.442	74.889	74.794	38	0.656	296.770	70.653	20.868	108.280	107.470	25	0.673	0.716
matern32 + quasinewton and Blue PC Features	345.890	50.520	9.626	93.177	92.918	38	0.656	297.390	70.417	20.893	108.250	107.370	25	0.683	0.868
matern32 + lbfgs and Blue PC Features	345.890	50.520	9.626	93.177	92.918	38	0.656	297.390	70.417	20.893	108.250	107.370	25	0.683	0.769
matern52 + quasinewton and Blue PC Features	366.830	53.754	10.211	94.990	94.697	38	0.656	297.720	70.165	20.909	108.240	107.340	25	0.683	0.715
matern52 + lbfgs and Blue PC Features	366.840	53.754	10.211	94.990	94.697	38	0.656	297.720	70.165	20.909	108.240	107.340	25	0.683	0.667
rationalquadratic + quasinewton and Blue PC Features	700.410	101.640	19.349	108.530	108.530	128	0.663	296.240	66.644	20.786	108.530	108.530	18	0.692	0.632
rationalquadratic + lbfgs and Blue PC Features	700.410	101.640	19.349	108.530	108.530	1	0.663	296.240	66.644	20.786	108.530	108.530	1	0.692	0.781
ardexponential + quasinewton and Blue PC Features	214.630	32.981	5.988	77.608	77.397	55	0.645	306.740	78.192	21.854	108.300	106.590	25	0.663	3.022
ardexponential + lbfgs and Blue PC Features	214.630	32.981	5.988	77.608	77.397	55	0.645	306.740	78.192	21.854	108.300	106.590	25	0.663	2.703
ardsquaredexponential + quasinewton and Blue PC Features	654.720	97.462	18.187	108.120	107.490	28	0.647	295.200	69.561	21.047	108.350	107.610	18	0.683	1.890
ardsquaredexponential + lbfgs and Blue PC Features	654.720	97.462	18.187	108.120	107.490	28	0.647	295.200	69.561	21.047	108.350	107.610	18	0.683	2.538
ardmatern32 + quasinewton and Blue PC Features	352.520	54.402	9.838	93.545	93.040	55	0.647	307.620	78.179	21.888	108.270	106.450	25	0.663	2.745
ardmatern32 + lbfgs and Blue PC Features	352.520	54.402	9.838	93.545	93.040	55	0.647	307.620	78.179	21.888	108.270	106.450	25	0.663	2.261

ardmatern52 + quasineutron and Blue PC Features	373.620	57.636	10.425	95.328	94.764	55	0.647	308.070	77.998	21.903	108.250	106.400	25	0.663	2.907
ardmatern52 + lbfgs and Blue PC Features	373.620	57.636	10.425	95.328	94.764	55	0.647	308.070	77.998	21.903	108.250	106.400	25	0.663	2.959
ardrationalquadratic + quasineutron and Blue PC Features	393.200	60.337	10.959	96.836	96.221	8	0.642	309.220	77.247	21.951	108.180	106.350	25	0.663	4.261
ardrationalquadratic + lbfgs and Blue PC Features	393.210	60.337	10.959	96.836	96.221	8	0.642	309.220	77.247	21.951	108.180	106.350	25	0.663	4.219
exponential + quasineutron and Blue PC Points	350.200	101.640	19.349	108.530	108.530	1	0.663	148.120	66.644	20.786	108.530	108.530	1	0.692	0.042
exponential + lbfgs and Blue PC Points	350.200	101.640	19.349	108.530	108.530	1	0.663	148.120	66.644	20.786	108.530	108.530	1	0.692	0.063
matern32 + quasineutron and Blue PC Points	350.200	101.640	19.349	108.530	108.530	157	0.663	148.120	66.644	20.786	108.530	108.530	13	0.692	0.037
matern32 + lbfgs and Blue PC Points	350.190	101.640	19.348	108.530	108.530	1	0.663	148.120	66.644	20.786	108.530	108.530	1	0.692	0.064
matern52 + quasineutron and Blue PC Points	350.200	101.640	19.349	108.530	108.530	157	0.663	148.120	66.644	20.786	108.530	108.530	13	0.692	0.034
matern52 + lbfgs and Blue PC Points	350.200	101.640	19.349	108.530	108.530	1	0.663	148.120	66.644	20.786	108.530	108.530	1	0.692	0.041
rationalquadratic + quasineutron and Blue PC Points	350.200	101.640	19.349	108.530	108.530	157	0.663	148.120	66.644	20.786	108.530	108.530	13	0.692	0.045
rationalquadratic + lbfgs and Blue PC Points	350.200	101.640	19.349	108.530	108.530	1	0.663	148.120	66.644	20.786	108.530	108.530	1	0.692	0.064
ardexponential + quasineutron and Blue PC Points	161.320	46.494	9.017	90.298	89.529	139	0.656	152.910	68.780	21.555	108.190	104.410	13	0.654	0.165
ardexponential + lbfgs and Blue PC Points	161.320	46.495	9.017	90.299	89.529	139	0.656	152.910	68.780	21.555	108.190	104.410	13	0.654	0.160
ardsquareexponential + quasineutron and Blue PC Points	319.070	95.816	18.287	108.900	105.970	139	0.644	140.590	64.164	20.067	109.120	105.930	13	0.615	0.078
ardsquareexponential + lbfgs and Blue PC Points	319.070	95.816	18.287	108.900	105.970	139	0.644	140.590	64.164	20.067	109.120	105.930	13	0.615	0.070
ardmatern32 + quasineutron and Blue PC Points	187.040	53.271	10.420	94.710	93.429	139	0.650	156.220	69.355	22.094	108.220	103.210	13	0.654	0.140
ardmatern32 + lbfgs and Blue PC Points	187.040	53.271	10.420	94.710	93.429	139	0.650	156.220	69.355	22.094	108.220	103.210	13	0.654	0.162
ardmatern52 + quasineutron and Blue PC Points	188.190	53.308	10.480	94.787	93.374	139	0.638	157.770	69.456	22.319	108.210	102.710	7	0.654	0.156
ardmatern52 + lbfgs and Blue PC Points	188.190	53.308	10.480	94.787	93.374	139	0.638	157.770	69.456	22.319	108.210	102.710	7	0.654	0.128
ardrationalquadratic + quasineutron and Blue PC Points	185.960	52.106	10.336	94.171	92.624	63	0.638	160.870	69.186	22.660	108.040	101.790	7	0.615	0.229
ardrationalquadratic + lbfgs and Blue PC Points	185.960	52.106	10.336	94.171	92.624	63	0.638	160.870	69.186	22.660	108.040	101.790	7	0.615	0.312
exponential + quasineutron and Green Features	0.071	0.011	0.002	1.542	1.541	97	0.666	294.680	66.370	20.948	108.400	107.490	16	0.673	1.642
exponential + lbfgs and Green Features	0.071	0.011	0.002	1.537	1.536	160	0.666	294.680	66.370	20.948	108.400	107.490	16	0.673	1.418
matern32 + quasineutron and Green Features	0.076	0.012	0.002	1.583	1.583	34	0.672	295.240	66.419	20.909	108.450	107.560	16	0.654	1.490
matern32 + lbfgs and Green Features	0.071	0.011	0.002	1.536	1.536	22	0.672	295.240	66.419	20.909	108.450	107.560	16	0.654	1.489
matern52 + quasineutron and Green Features	32.125	4.990	0.893	32.240	32.229	34	0.669	295.430	66.399	20.898	108.480	107.610	16	0.654	1.086
matern52 + lbfgs and Green Features	32.125	4.990	0.893	32.240	32.228	34	0.669	295.430	66.399	20.898	108.480	107.610	16	0.654	0.899
rationalquadratic + quasineutron and Green Features	0.076	0.012	0.002	1.586	1.586	34	0.670	294.640	66.145	20.932	108.440	107.500	16	0.663	2.202
rationalquadratic + lbfgs and Green Features	0.071	0.011	0.002	1.536	1.536	34	0.670	294.640	66.145	20.932	108.440	107.500	16	0.663	1.916
ardexponential + quasineutron and Green Features	0.074	0.011	0.002	1.536	1.536	22	0.644	316.210	74.953	22.920	108.120	102.040	1	0.644	159.580
ardexponential + lbfgs and Green Features	0.074	0.011	0.002	1.536	1.536	98	0.642	309.700	68.997	22.380	107.790	103.060	1	0.654	77.498
ardsquareexponential + quasineutron and Green Features	0.078	0.013	0.002	1.536	1.536	42	0.633	312.470	76.802	22.592	109.250	103.510	1	0.644	168.480
ardsquareexponential + lbfgs and Green Features	0.077	0.014	0.002	1.536	1.536	153	0.655	307.260	79.768	21.851	108.820	103.860	6	0.644	178.400
ardmatern32 + quasineutron and Green Features	0.076	0.012	0.002	1.536	1.536	22	0.639	326.010	83.854	23.990	108.620	100.550	1	0.615	81.472
ardmatern32 + lbfgs and Green Features	0.075	0.011	0.002	1.536	1.536	22	0.652	307.620	71.125	22.163	107.950	102.910	26	0.606	207.310
ardmatern52 + quasineutron and Green Features	0.076	0.011	0.002	1.536	1.536	98	0.639	315.940	78.234	22.930	108.910	101.070	1	0.663	176.300
ardmatern52 + lbfgs and Green Features	0.075	0.011	0.002	1.536	1.536	22	0.633	296.690	68.530	21.792	107.830	102.570	1	0.654	262.300
ardrationalquadratic + quasineutron and Green Features	0.081	0.019	0.002	1.536	1.536	94	0.623	300.030	73.716	21.535	110.030	99.605	1	0.625	137.280
ardrationalquadratic + lbfgs and Green Features	0.082	0.019	0.002	1.536	1.536	34	0.627	294.470	68.912	20.991	110.060	99.533	1	0.635	229.550
exponential + quasineutron and Green Points	0.045	0.013	0.002	1.768	1.744	157	0.663	147.340	66.727	20.696	108.490	108.480	7	0.692	0.151
exponential + lbfgs and Green Points	0.035	0.010	0.002	1.580	1.541	157	0.663	147.340	66.727	20.696	108.490	108.480	7	0.692	0.134
matern32 + quasineutron and Green Points	0.083	0.024	0.005	2.360	2.360	157	0.663	147.200	66.749	20.686	108.470	108.460	7	0.692	0.166
matern32 + lbfgs and Green Points	0.035	0.010	0.002	1.540	1.540	157	0.663	147.200	66.749	20.686	108.470	108.460	7	0.692	0.144
matern52 + quasineutron and Green Points	0.244	0.071	0.013	4.051	4.051	159	0.663	147.260	66.750	20.695	108.470	108.460	7	0.692	0.140
matern52 + lbfgs and Green Points	0.044	0.013	0.002	1.722	1.722	3	0.663	147.260	66.750	20.695	108.470	108.460	7	0.692	0.121
rationalquadratic + quasineutron and Green Points	350.190	101.640	19.349	108.530	108.530	3	0.663	148.120	66.644	20.786	108.530	108.530	7	0.692	0.064
rationalquadratic + lbfgs and Green Points	0.035	0.010	0.002	1.541	1.541	60	0.669	147.650	66.751	20.738	108.450	108.450	1	0.692	0.414
ardexponential + quasineutron and Green Points	0.040	0.010	0.002	1.540	1.540	157	0.606	128.400	62.867	17.247	106.520	92.801	14	0.692	0.847
ardexponential + lbfgs and Green Points	0.039	0.010	0.002	1.540	1.540	157	0.606	124.180	62.699	16.855	107.600	96.108	14	0.654	0.536

ardsquaredexponential + quasinewton and Green Points	0.042	0.012	0.002	1.540	1.540	157	0.600	146.270	70.391	20.797	105.360	88.109	6	0.692	0.642
ardsquaredexponential + lbfgs and Green Points	0.043	0.014	0.002	1.540	1.540	157	0.606	147.960	70.822	21.118	105.940	87.690	6	0.615	1.512
ardmatern32 + quasinewton and Green Points	0.040	0.011	0.002	1.540	1.540	157	0.638	134.730	66.021	19.051	105.800	90.983	6	0.654	0.828
ardmatern32 + lbfgs and Green Points	0.040	0.010	0.002	1.540	1.540	157	0.631	132.660	69.953	18.811	104.700	91.399	6	0.615	0.602
ardmatern52 + quasinewton and Green Points	0.040	0.012	0.002	1.540	1.540	157	0.644	164.630	92.325	21.898	105.090	94.745	14	0.692	0.589
ardmatern52 + lbfgs and Green Points	0.041	0.010	0.002	1.540	1.540	157	0.613	138.040	72.202	19.551	105.050	90.247	6	0.654	0.640
ardrationalquadratic + quasinewton and Green Points	0.042	0.011	0.003	1.540	1.540	157	0.563	169.970	73.171	26.164	108.720	82.834	14	0.577	0.726
ardrationalquadratic + lbfgs and Green Points	0.042	0.011	0.003	1.540	1.540	157	0.563	169.970	73.171	26.164	108.720	82.834	14	0.577	0.719
exponential + quasinewton and Green PC Features	597.540	89.854	16.632	107.210	106.920	71	0.658	295.670	67.151	20.689	108.410	108.040	12	0.663	0.672
exponential + lbfgs and Green PC Features	597.540	89.854	16.632	107.210	106.920	71	0.658	295.670	67.151	20.689	108.410	108.040	12	0.663	0.502
matern32 + quasinewton and Green PC Features	645.540	97.101	17.971	108.080	107.740	17	0.656	295.410	67.124	20.682	108.430	108.040	12	0.663	0.474
matern32 + lbfgs and Green PC Features	645.540	97.101	17.971	108.080	107.740	17	0.656	295.410	67.124	20.682	108.430	108.040	12	0.663	0.359
matern52 + quasinewton and Green PC Features	654.020	98.359	18.208	108.190	107.830	17	0.656	295.310	67.098	20.679	108.440	108.040	12	0.663	0.437
matern52 + lbfgs and Green PC Features	654.020	98.359	18.208	108.190	107.830	17	0.656	295.310	67.098	20.679	108.440	108.040	12	0.663	0.407
rationalquadratic + quasinewton and Green PC Features	0.338	0.050	0.009	3.363	3.363	71	0.658	295.750	66.859	20.751	108.260	108.000	25	0.663	3.015
rationalquadratic + lbfgs and Green PC Features	0.070	0.010	0.002	1.536	1.536	71	0.658	295.750	66.859	20.751	108.260	108.000	25	0.663	3.083
ardexponential + quasinewton and Green PC Features	527.870	82.261	14.726	104.890	104.370	80	0.645	297.690	70.660	20.962	108.360	107.430	25	0.663	2.252
ardexponential + lbfgs and Green PC Features	450.300	67.537	12.514	101.010	100.740	137	0.655	295.480	70.665	20.574	108.210	107.600	18	0.663	3.382
ardsquaredexponential + quasinewton and Green PC Features	624.810	97.771	17.431	107.700	106.880	80	0.647	298.270	70.394	20.985	108.430	107.310	17	0.654	2.316
ardsquaredexponential + lbfgs and Green PC Features	624.810	97.771	17.431	107.700	106.880	80	0.647	298.270	70.394	20.985	108.430	107.310	17	0.654	2.708
ardmatern32 + quasinewton and Green PC Features	599.650	93.522	16.733	107.160	106.500	80	0.647	297.580	70.454	20.956	108.380	107.420	17	0.663	2.257
ardmatern32 + lbfgs and Green PC Features	599.650	93.522	16.733	107.160	106.500	80	0.647	297.580	70.454	20.956	108.380	107.420	17	0.663	2.549
ardmatern52 + quasinewton and Green PC Features	613.840	95.672	17.126	107.480	106.770	80	0.647	297.570	70.326	20.955	108.390	107.410	17	0.663	2.674
ardmatern52 + lbfgs and Green PC Features	613.840	95.672	17.126	107.480	106.770	80	0.647	297.570	70.326	20.955	108.390	107.410	17	0.663	2.158
ardrationalquadratic + quasinewton and Green PC Features	624.800	97.770	17.431	107.700	106.880	80	0.647	298.270	70.394	20.985	108.430	107.310	17	0.654	3.691
ardrationalquadratic + lbfgs and Green PC Features	0.072	0.010	0.002	1.536	1.536	127	0.661	295.740	66.114	20.753	108.680	107.910	1	0.644	8.695
exponential + quasinewton and Green PC Points	350.200	101.640	19.349	108.530	108.530	7	0.663	148.120	66.644	20.786	108.530	108.530	7	0.692	0.033
exponential + lbfgs and Green PC Points	350.200	101.640	19.349	108.530	108.530	1	0.663	148.120	66.644	20.786	108.530	108.530	1	0.692	0.042
matern32 + quasinewton and Green PC Points	350.200	101.640	19.349	108.530	108.530	157	0.663	148.120	66.644	20.786	108.530	108.530	14	0.692	0.033
matern32 + lbfgs and Green PC Points	350.200	101.640	19.349	108.530	108.530	9	0.663	148.120	66.644	20.786	108.530	108.530	7	0.692	0.043
matern52 + quasinewton and Green PC Points	350.200	101.640	19.349	108.530	108.530	157	0.663	148.120	66.644	20.786	108.530	108.530	14	0.692	0.042
matern52 + lbfgs and Green PC Points	350.200	101.640	19.349	108.530	108.530	157	0.663	148.120	66.644	20.786	108.530	108.530	14	0.692	0.059
rationalexponential + quasinewton and Green PC Points	350.200	101.640	19.349	108.530	108.530	157	0.663	148.120	66.644	20.786	108.530	108.530	14	0.692	0.055
rationalexponential + lbfgs and Green PC Points	350.200	101.640	19.349	108.530	108.530	1	0.663	148.120	66.644	20.786	108.530	108.530	1	0.692	0.070
ardexponential + quasinewton and Green PC Points	0.046	0.012	0.003	1.744	1.744	58	0.656	152.100	71.140	21.342	107.750	106.890	14	0.692	0.345
ardexponential + lbfgs and Green PC Points	0.036	0.010	0.002	1.540	1.540	58	0.656	152.100	71.139	21.342	107.750	106.890	14	0.692	0.306
ardsquaredexponential + quasinewton and Green PC Points	332.440	99.659	18.635	108.900	107.190	49	0.650	146.600	67.521	20.760	109.090	107.210	14	0.654	0.134
ardsquaredexponential + lbfgs and Green PC Points	332.440	99.659	18.635	108.900	107.190	49	0.650	146.600	67.521	20.760	109.090	107.210	14	0.654	0.144
ardmatern32 + quasinewton and Green PC Points	312.470	92.362	17.482	107.810	106.660	49	0.656	154.280	68.385	21.568	108.600	107.080	7	0.654	0.264
ardmatern32 + lbfgs and Green PC Points	319.950	93.923	17.897	108.080	107.000	49	0.669	155.380	69.192	21.710	108.600	107.230	7	0.654	0.212
ardmatern52 + quasinewton and Green PC Points	332.660	99.613	18.629	108.880	107.340	49	0.650	147.720	67.885	20.862	109.070	107.370	14	0.654	0.144
ardmatern52 + lbfgs and Green PC Points	332.660	99.613	18.629	108.880	107.340	49	0.650	147.720	67.885	20.862	109.070	107.370	14	0.654	0.169
ardrationalquadratic + quasinewton and Green PC Points	312.020	92.414	17.484	107.820	106.360	49	0.669	154.320	67.259	21.601	108.680	106.750	7	0.654	0.229
ardrationalquadratic + lbfgs and Green PC Points	318.710	93.541	17.869	108.060	106.710	49	0.669	155.980	68.377	21.843	108.660	106.930	7	0.654	0.167
exponential + quasinewton and Red Features	0.074	0.011	0.002	1.560	1.559	159	0.652	290.140	71.269	20.549	108.180	106.810	18	0.644	1.632
exponential + lbfgs and Red Features	0.071	0.011	0.002	1.537	1.536	88	0.652	290.140	71.269	20.549	108.180	106.810	18	0.644	1.633
matern32 + quasinewton and Red Features	0.072	0.010	0.002	1.544	1.544	34	0.656	291.570	70.761	20.605	108.080	107.130	18	0.663	1.840
matern32 + lbfgs and Red Features	0.071	0.010	0.002	1.536	1.536	22	0.656	291.570	70.761	20.605	108.080	107.130	18	0.663	1.448
matern52 + quasinewton and Red Features	0.072	0.010	0.002	1.544	1.544	22	0.656	292.270	70.337	20.647	108.060	107.270	18	0.683	1.324
matern52 + lbfgs and Red Features	0.071	0.010	0.002	1.536	1.536	22	0.656	292.270	70.337	20.647	108.060	107.270	18	0.683	1.351

rationalquadratic + quasinewton and Red Features	0.072	0.010	0.002	1.539	1.539	34	0.650	289.720	70.520	20.524	108.030	106.760	18	0.635	1.871
rationalquadratic + lbfsgs and Red Features	0.071	0.010	0.002	1.536	1.536	34	0.650	289.720	70.520	20.524	108.030	106.760	18	0.635	2.172
ardexponential + quasinewton and Red Features	0.074	0.011	0.002	1.536	1.536	3	0.636	296.420	72.994	22.150	108.450	102.240	19	0.596	80.589
ardexponential + lbfsgs and Red Features	0.073	0.012	0.002	1.536	1.536	40	0.638	293.400	75.715	21.291	107.490	104.080	18	0.644	180.210
ardsquaredexponential + quasinewton and Red Features	0.078	0.011	0.002	1.536	1.536	40	0.644	315.430	74.013	23.355	107.790	99.824	12	0.625	161.160
ardsquaredexponential + lbfsgs and Red Features	0.078	0.012	0.002	1.536	1.536	40	0.648	312.290	77.925	23.281	107.980	100.680	14	0.596	280.010
ardmatern32 + quasinewton and Red Features	0.076	0.010	0.002	1.536	1.536	111	0.644	312.860	73.957	23.532	108.470	101.030	14	0.635	98.444
ardmatern32 + lbfsgs and Red Features	0.074	0.012	0.002	1.536	1.536	42	0.631	287.740	76.275	20.645	107.240	103.070	16	0.625	213.650
ardmatern52 + quasinewton and Red Features	0.077	0.010	0.002	1.536	1.536	40	0.644	317.070	71.488	23.986	108.460	100.670	14	0.635	130.960
ardmatern52 + lbfsgs and Red Features	0.076	0.015	0.002	1.536	1.536	40	0.634	296.010	80.478	21.385	108.040	102.370	14	0.596	137.660
ardrationalquadratic + quasinewton and Red Features	0.077	0.011	0.002	1.536	1.536	40	0.639	291.630	81.291	20.708	107.660	102.230	18	0.654	123.680
ardrationalquadratic + lbfsgs and Red Features	0.075	0.010	0.002	1.536	1.536	28	0.639	288.430	72.322	21.016	107.920	103.170	18	0.625	153.660
exponential + quasinewton and Red Points	344.270	99.827	19.030	108.510	108.510	157	0.663	148.050	66.795	20.751	108.530	108.520	22	0.692	0.413
exponential + lbfsgs and Red Points	344.270	99.827	19.030	108.510	108.510	122	0.663	148.050	66.795	20.751	108.530	108.520	22	0.692	0.172
matern32 + quasinewton and Red Points	346.700	100.510	19.166	108.520	108.520	157	0.663	148.020	66.813	20.740	108.530	108.520	22	0.692	0.104
matern32 + lbfsgs and Red Points	348.140	101.040	19.235	108.530	108.530	9	0.663	148.120	66.644	20.786	108.530	108.530	1	0.692	0.120
matern52 + quasinewton and Red Points	348.750	101.220	19.269	108.530	108.530	1	0.663	148.120	66.644	20.786	108.530	108.530	1	0.692	0.217
matern52 + lbfsgs and Red Points	349.370	101.400	19.303	108.530	108.530	1	0.663	148.120	66.644	20.786	108.530	108.530	1	0.692	0.146
rationalquadratic + quasinewton and Red Points	350.070	101.600	19.342	108.530	108.530	157	0.663	148.120	66.644	20.785	108.530	108.530	22	0.692	0.086
rationalquadratic + lbfsgs and Red Points	347.410	100.670	19.212	108.520	108.510	122	0.663	147.930	66.835	20.706	108.530	108.520	22	0.692	0.123
ardexponential + quasinewton and Red Points	0.043	0.012	0.003	1.540	1.540	137	0.619	169.630	70.161	26.235	103.720	85.266	14	0.577	0.874
ardexponential + lbfsgs and Red Points	0.043	0.012	0.003	1.540	1.540	137	0.625	169.520	70.384	26.159	103.820	85.388	14	0.577	0.570
ardsquaredexponential + quasinewton and Red Points	0.046	0.015	0.003	1.540	1.540	52	0.613	178.610	81.065	26.380	111.400	78.578	14	0.654	0.669
ardsquaredexponential + lbfsgs and Red Points	0.046	0.015	0.003	1.540	1.540	52	0.613	178.610	81.065	26.380	111.400	78.578	14	0.654	0.586
ardmatern32 + quasinewton and Red Points	0.046	0.014	0.003	1.540	1.540	137	0.606	178.610	77.201	27.533	105.730	79.789	14	0.577	0.748
ardmatern32 + lbfsgs and Red Points	0.047	0.015	0.003	1.540	1.540	137	0.619	179.250	77.649	27.635	106.040	79.856	14	0.577	0.569
ardmatern52 + quasinewton and Red Points	19.205	5.616	1.126	30.966	30.683	137	0.625	177.170	73.333	28.026	107.100	78.700	12	0.577	1.904
ardmatern52 + lbfsgs and Red Points	0.046	0.014	0.003	1.540	1.540	137	0.650	185.870	83.468	27.599	109.220	81.685	14	0.615	0.716
ardrationalquadratic + quasinewton and Red Points	0.046	0.014	0.003	1.540	1.540	137	0.631	178.470	78.473	27.387	106.020	78.481	14	0.615	1.214
ardrationalquadratic + lbfsgs and Red Points	0.047	0.014	0.003	1.540	1.540	137	0.619	171.570	74.218	26.469	106.320	83.224	14	0.577	0.620
exponential + quasinewton and Red PC Features	629.120	93.060	17.690	107.720	106.570	34	0.648	291.150	69.977	20.823	108.350	106.910	18	0.654	0.415
exponential + lbfsgs and Red PC Features	629.120	93.060	17.690	107.720	106.570	34	0.648	291.150	69.977	20.823	108.350	106.910	18	0.654	0.335
matern32 + quasinewton and Red PC Features	655.350	96.504	18.456	108.180	106.810	34	0.647	290.970	69.774	20.807	108.430	106.830	18	0.654	0.360
matern32 + lbfsgs and Red PC Features	655.350	96.504	18.456	108.180	106.810	34	0.647	290.970	69.774	20.807	108.430	106.830	18	0.654	0.294
matern52 + quasinewton and Red PC Features	659.770	96.982	18.598	108.270	106.810	34	0.642	290.970	69.754	20.805	108.470	106.790	18	0.654	0.357
matern52 + lbfsgs and Red PC Features	659.770	96.982	18.598	108.270	106.810	34	0.642	290.970	69.754	20.805	108.470	106.790	18	0.654	0.298
rationalquadratic + quasinewton and Red PC Features	664.350	97.477	18.765	108.410	106.740	34	0.645	291.230	70.644	20.816	108.560	106.670	18	0.663	0.817
rationalquadratic + lbfsgs and Red PC Features	664.350	97.477	18.765	108.410	106.740	34	0.645	291.230	70.644	20.816	108.560	106.670	18	0.663	1.212
ardexponential + quasinewton and Red PC Features	598.100	88.181	16.904	106.750	105.480	34	0.636	302.370	71.524	21.616	107.930	106.270	18	0.644	2.126
ardexponential + lbfsgs and Red PC Features	598.100	88.181	16.904	106.750	105.480	34	0.636	302.370	71.524	21.616	107.930	106.270	18	0.644	3.146
ardsquaredexponential + quasinewton and Red PC Features	652.910	96.283	18.466	107.860	106.260	34	0.641	301.090	72.001	21.571	108.020	106.260	18	0.663	1.631
ardsquaredexponential + lbfsgs and Red PC Features	652.910	96.283	18.466	107.860	106.260	34	0.641	301.090	72.001	21.571	108.020	106.260	18	0.663	2.482
ardmatern32 + quasinewton and Red PC Features	634.830	93.797	17.946	107.520	106.080	34	0.641	302.440	71.613	21.628	107.960	106.280	18	0.654	2.009
ardmatern32 + lbfsgs and Red PC Features	634.830	93.797	17.946	107.520	106.080	34	0.641	302.440	71.613	21.628	107.960	106.280	18	0.654	2.525
ardmatern52 + quasinewton and Red PC Features	642.280	94.958	18.157	107.650	106.170	34	0.638	302.200	71.699	21.622	107.970	106.280	18	0.663	1.641
ardmatern52 + lbfsgs and Red PC Features	642.280	94.959	18.157	107.650	106.170	34	0.638	302.200	71.699	21.622	107.970	106.280	18	0.663	2.493
ardrationalquadratic + quasinewton and Red PC Features	636.640	94.043	17.997	107.510	106.130	34	0.641	302.890	71.362	21.618	107.940	106.320	18	0.654	2.532
ardrationalquadratic + lbfsgs and Red PC Features	636.660	94.045	17.998	107.510	106.130	34	0.641	302.890	71.363	21.618	107.940	106.320	18	0.654	4.021
exponential + quasinewton and Red PC Points	350.200	101.640	19.349	108.530	108.530	122	0.663	148.120	66.644	20.785	108.530	108.530	22	0.692	0.036
exponential + lbfsgs and Red PC Points	350.200	101.640	19.349	108.530	108.530	1	0.663	148.120	66.644	20.786	108.530	108.530	1	0.692	0.040
matern32 + quasinewton and Red PC Points	350.200	101.640	19.349	108.530	108.530	157	0.663	148.120	66.644	20.786	108.530	108.530	22	0.692	0.033

matern32 + lbfgs and Red PC Points	350.200	101.640	19.349	108.530	108.530	1	0.663	148.120	66.644	20.786	108.530	108.530	1	0.692	0.046
matern52 + quasinewton and Red PC Points	350.200	101.640	19.349	108.530	108.530	3	0.663	148.120	66.644	20.786	108.530	108.530	13	0.692	0.036
matern52 + lbfgs and Red PC Points	350.200	101.640	19.349	108.530	108.530	122	0.663	148.120	66.644	20.785	108.530	108.530	22	0.692	0.064
rationalquadratic + quasinewton and Red PC Points	350.200	101.640	19.349	108.530	108.530	157	0.663	148.120	66.644	20.786	108.530	108.530	14	0.692	0.044
rationalquadratic + lbfgs and Red PC Points	350.200	101.640	19.349	108.530	108.530	3	0.663	148.120	66.644	20.786	108.530	108.530	2	0.692	0.060
ardexponential + quasinewton and Red PC Points	342.380	99.554	18.985	108.640	108.300	139	0.663	146.040	65.652	20.132	108.680	108.330	22	0.654	0.225
ardexponential + lbfgs and Red PC Points	350.200	101.640	19.349	108.530	108.530	1	0.663	148.120	66.644	20.786	108.530	108.530	1	0.692	0.092
ardsquaredexponential + quasinewton and Red PC Points	341.160	99.495	18.976	109.020	107.820	139	0.656	146.260	65.544	20.104	109.050	107.870	22	0.654	0.117
ardsquaredexponential + lbfgs and Red PC Points	341.160	99.495	18.976	109.020	107.820	139	0.656	146.260	65.544	20.105	109.050	107.870	22	0.654	0.142
ardmatern32 + quasinewton and Red PC Points	342.030	99.562	18.998	108.860	108.060	139	0.656	145.880	65.409	20.045	108.890	108.100	22	0.654	0.147
ardmatern32 + lbfgs and Red PC Points	342.030	99.562	18.998	108.860	108.060	139	0.656	145.880	65.408	20.045	108.890	108.100	22	0.654	0.163
ardmatern52 + quasinewton and Red PC Points	341.740	99.529	18.992	108.930	107.970	139	0.663	145.970	65.385	20.065	108.970	108.010	22	0.654	0.130
ardmatern52 + lbfgs and Red PC Points	341.740	99.529	18.992	108.930	107.970	139	0.663	145.970	65.385	20.065	108.970	108.010	22	0.654	0.157
ardrationalquadratic + quasinewton and Red PC Points	341.160	99.495	18.976	109.020	107.820	139	0.656	146.260	65.544	20.105	109.050	107.870	22	0.654	0.228
ardrationalquadratic + lbfgs and Red PC Points	341.160	99.495	18.976	109.020	107.820	139	0.656	146.260	65.544	20.105	109.050	107.870	22	0.654	0.318